



**The Abdus Salam
International Centre for Theoretical Physics**



2060-54

**Advanced School on Non-linear Dynamics and Earthquake
Prediction**

28 September - 10 October, 2009

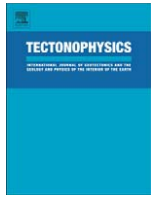
Can Earth's rotation and tidal despinning drive plate tectonics?

C. Doglioni
*Dipartimento di Scienze della Terra
Università La Sapienza
Rome
Italy*



Contents lists available at ScienceDirect

Tectonophysics

journal homepage: www.elsevier.com/locate/tecto

Can Earth's rotation and tidal despinning drive plate tectonics?

Federica Riguzzi ^{a,c,*}, Giuliano Panza ^b, Peter Varga ^d, Carlo Doglioni ^{a,*}

^a Dipartimento di Scienze della Terra, Università Sapienza, Roma, Italy

^b Dipartimento di Scienze della Terra, Università di Trieste, and ICTP, Italy

^c Istituto Nazionale di Geofisica e Vulcanologia, Roma, Italy

^d Geodetic and Geophysical Research Institute, Seismological Observatory, Budapest, Hungary

ARTICLE INFO

Article history:

Received 9 January 2009

Accepted 10 June 2009

Available online xxxx

Keywords:

Plate tectonics

Earth's rotation

Tidal despinning

Earth's energy budget

ABSTRACT

We re-evaluate the possibility that Earth's rotation contributes to plate tectonics on the basis of the following observations: 1) plates move along a westerly polarized flow that forms an angle relative to the equator close to the revolution plane of the Moon; 2) plate boundaries are asymmetric, being their geographic polarity the first order controlling parameter; unlike recent analysis, the slab dip is confirmed to be steeper along W-directed subduction zones; 3) the global seismicity depends on latitude and correlates with the decadal oscillations of the excess length of day (LOD); 4) the Earth's deceleration supplies energy to plate tectonics comparable to the computed budget dissipated by the deformation processes; 5) the Gutenberg–Richter law supports that the whole lithosphere is a self-organized system in critical state, i.e., a force is acting contemporaneously on all the plates and distributes the energy over the whole lithospheric shell, a condition that can be satisfied by a force acting at the astronomical scale.

Assuming an ultra-low viscosity layer in the upper asthenosphere, the horizontal component of the tidal oscillation and torque would be able to slowly shift the lithosphere relative to the mantle.

© 2009 Elsevier B.V. All rights reserved.

1. Introduction

The energy budget of plate tectonics and the basic mechanisms that move plates are far to be entirely understood. A very large number of papers have suggested strong evidence for a system driven primarily by lateral density heterogeneities, controlled by the thermal cooling of the Earth, particularly with the cool slab pulling the attached plates (Conrad and Lithgow-Bertelloni, 2003). However, a number of issues contradict a simple thermal model capable to generate the Earth's geodynamics (Anderson, 1989). Large plates move coherently, being decoupled at the LVZ (Fig. 1). They show that the force acting on them is uniformly distributed and not concentrated to their margins. For example, the inferred slab pull would be stronger than the strength plates can sustain under extension (pull). Moreover, the geological and geophysical asymmetries of rift and subduction zones as a function of their polarity (Doglioni et al., 2007) may be interpreted as controlled by some astronomical mechanical shear (Scoppola et al., 2006).

The interest in the Earth's rotation as driving plate tectonics goes back to the theory of Wegener and to a number of papers in the early seventies (Bostrom, 1971; Knopoff and Leeds, 1972). This relation is based on the observation that plates have, for example, a westerly directed polarization relative to Antarctica (Le Pichon, 1968) or re-

lative to the hotspot reference frame (Ricard et al., 1991; Gripp and Gordon, 2002; Crespi et al., 2007).

In this article we review a number of topics about the rotational contribution to plate tectonics, finally proposing a mechanical model to explain it.

2. Evidences for a worldwide asymmetry

It has been shown how plate motions followed and follow a mainstream (Fig. 2) that can be reconstructed from ocean magnetic anomalies and space geodesy data (Doglioni, 1990; Crespi et al., 2007). This flow is polarized toward the “west” relative to the mantle. The net rotation is only an average value in the deep hotspot reference frame, but it rises to a complete polarization in the shallow hotspot reference frame (Fig. 2). The latitude range of the net rotation equator is about the same of the Moon maximum declination range ($\pm 28^\circ$) during the nutation period (≈ 18.6 yr). Further indications come from the fact that the induced geopotential variations and the solid Earth tide modeling (McCarthy and Petit, 2004) generate maximum amplitudes of the Earth bulges (≈ 30 cm) propagating progressively within the same latitude range. In particular, the track of the semidiurnal bulge crest is about directed from E to W, as small circles moving from latitudes 28° to 18° , when the Moon moves from maximum to minimum declinations (the same happens at negative latitudes for the opposite bulge), thus suggesting a role of rotational and tidal drag effects (Bostrom, 2000; Crespi et al., 2007).

* Corresponding authors.

E-mail addresses: riguzzi@ingv.it (F. Riguzzi), carlo.doglioni@uniroma1.it (C. Doglioni).

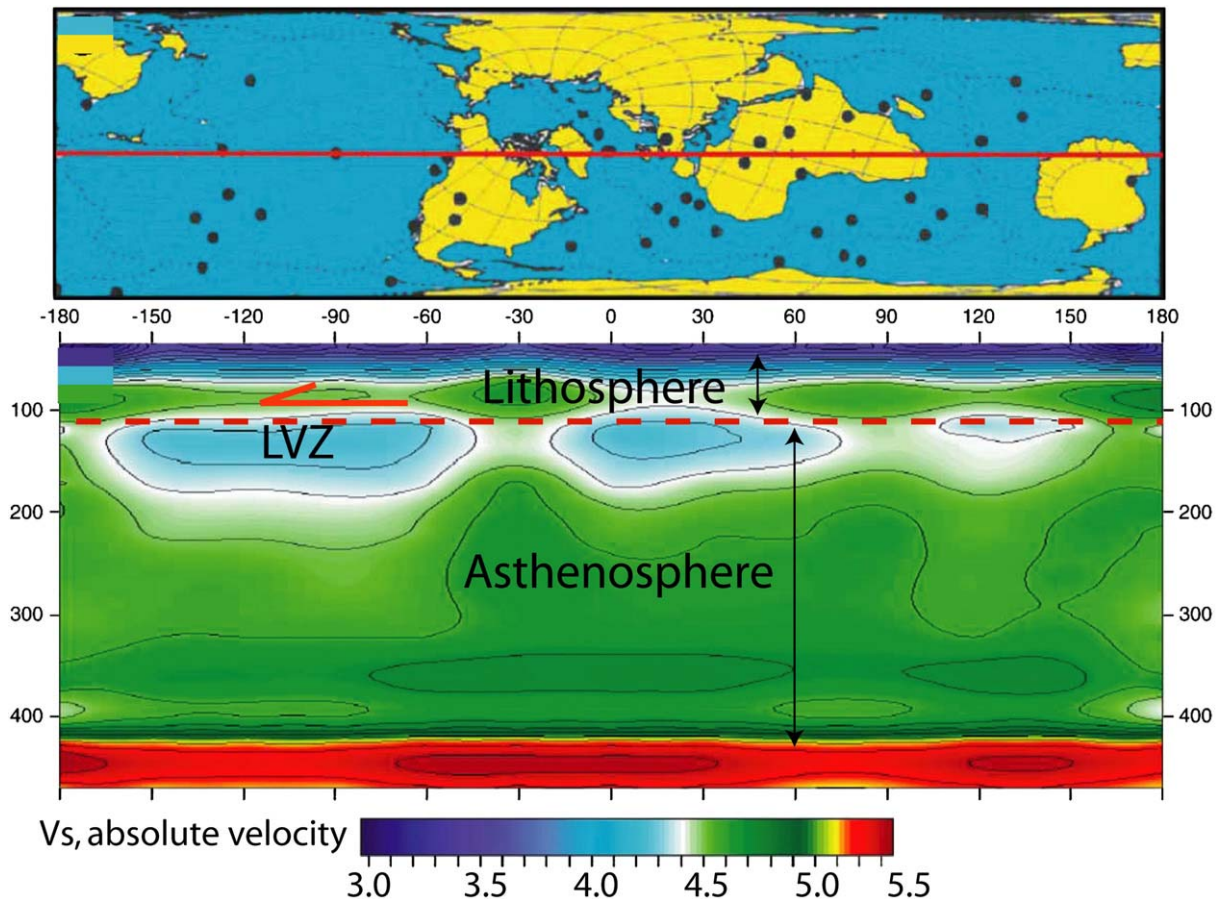


Fig. 1. Earth's cross section and related location map (red line, above), modified after Thybo (2006). Absolute shear wave velocity model includes a pronounced, global Low Velocity Zone (LVZ) at the top of the asthenosphere, which is strongest underneath the oceans, but also clearly identifiable underneath the continents. This level is here inferred as the main decoupling zone at the base of the lithosphere, possibly having an internal sub-layer with ultra-low viscosity, much lower than the average asthenosphere. (For interpretation of the references to color in this figure legend, the reader is referred to the web version of this article.)

Tectonic features on Earth show profound asymmetries as a function of their geographic polarity. A long list of signatures marks the distinction between orogens and related subduction zones and rift zones (Zhang and Tanimoto, 1993; Doglioni et al., 2003). These differences can be observed moving along the undulated flow of plate motions (Crespi et al., 2007; Doglioni et al., 2007) and diminish if east-versus west-facing structures are compared. The orogens associated with E- or NE-directed slabs (orogens of type A) are more elevated (>1000 m) with respect to what is observed at the steeper W-directed slabs, where the accretionary prisms (orogens of type B) have much lower average elevation (–1250 m), as shown in Fig. 3. The rocks outcropping along the orogens related to the E- or NE-directed subduction zones represent the entire crust and upper mantle section, whereas at the W-directed slab, the accretionary prisms are mostly composed by sedimentary and upper-crust rocks. Therefore orogens of type A have much deeper decoupling planes with respect to orogens of type B. The foredeep has lower subsidence rates (<0.2 mm/yr) along E- or NE-directed subduction zones with respect to the W-directed ones, where the foredeep-trench subsidence is much faster (>1 mm/yr). Along the E- or NE-directed subduction zones, the subduction hinge moves toward the upper plate, whereas it generally moves away from the upper plate along the W-directed subduction zones. This asymmetric behavior implies, on average, a three times faster lithospheric recycling into the mantle along W-directed subduction zones and provides evidence for polarized mantle convection. Gravity, heat flow anomalies, seismicity, etc. also support these differences, and along rift zones, the eastern flank is, on average, 100–300 m shallower than the western flank (Fig. 3).

Another critical issue is the dip of the subduction zones. The slab dip has been the topic of a number of researches (e.g., Jarrard, 1986). During the seventies it was noticed that the western Pacific slabs are steeper than the eastern side (Isacks and Barazangi, 1977). This asymmetry has been used (Nelson and Temple, 1972; Dickinson, 1978; Uyeda and Kanamori, 1979; Doglioni, 1990; 1993) to infer a mantle flow directed toward the “east”, confirming the notion of the “westerly” drift of the lithosphere (Le Pichon, 1968; Bostrom, 1971; Shaw and Jackson, 1973; Moore, 1973). Recently, Lallemand et al. (2005), based on a study where they divided each slab into a shallower part (<125 km) and a deeper segment (>125 km), suggested that the dip difference between western- and eastern-directed subduction zones is not statistically significant, but they recognized that the slabs beneath the oceanic crust are steeper than beneath the continents. This slope difference confirms the presence of a large asymmetry in the Pacific, where the less steep slabs with continental lithosphere lie along the eastern margin, whereas the generally steeper slabs (apart Japan) with oceanic lithosphere in the overriding plate, prevail along the western Pacific margins.

The westward drift of the lithosphere implies a relative “eastward” mantle flow (e.g. Panza et al., 2007), the decoupling taking place in the asthenosphere whose top, generally, is deeper than 100 km. Therefore the shallow part of the slab may not show any relevant dip difference.

Cruciani et al. (2005) carefully measured the slab dip and they demonstrated that the slab age is not correlated to the dip of the slab, contrary to earlier observations (e.g., Wortel, 1984). The analysis of Cruciani et al. (2005) is deliberately limited to the uppermost 250 km of depth because in E- or NE-directed subduction zones, seismicity

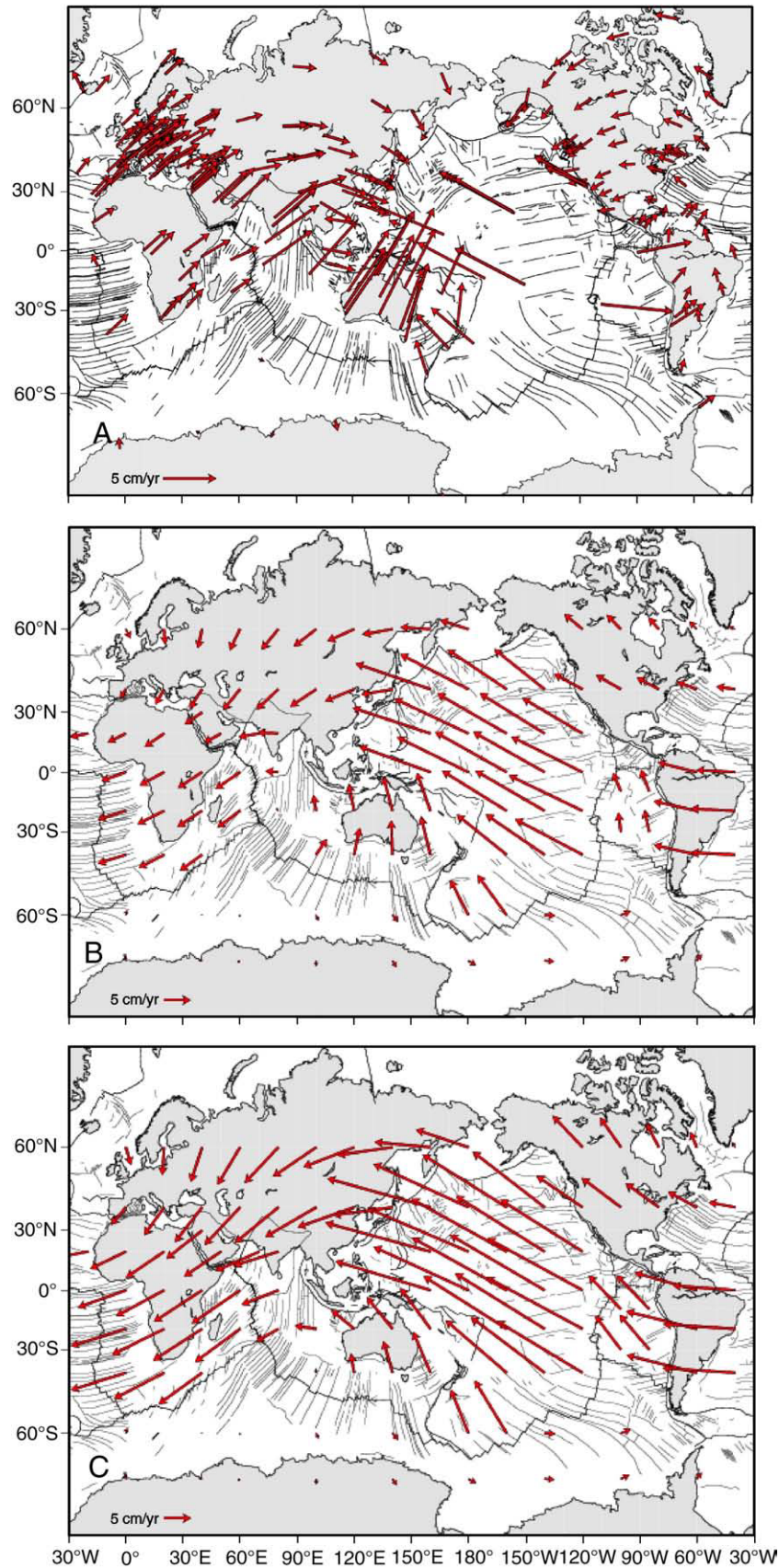


Fig. 2. Plate motions in the NNR reference frame (A, after [Altamimi et al., 2007](#)), in the deep (B) and shallow (C) hotspot reference frames ([Crespi et al., 2007](#)). In all reference frames plates follow an undulate mainstream. In case C, plates have a complete “westerly” directed polarization relative to the mantle.

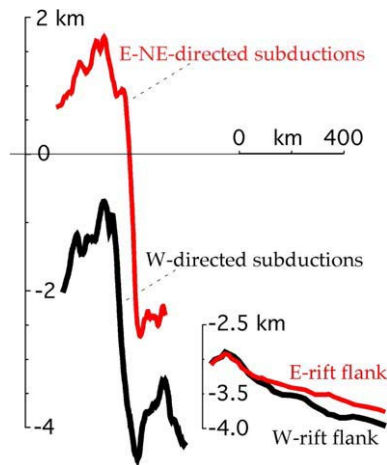


Fig. 3. Comparison between the average topography–bathymetry of subduction zones (left) and rift zones (right). The elevation is higher in the E- or NE-directed subduction zones and in the E-flank of rift zones.

does not extend systematically at greater depth, apart few areas where it appears concentrated between 550 and 670 km depth, close to the lower boundary of the upper mantle. The origin of these deep isolated earthquakes remains obscure: mineral phase change (Green and Houston, 1995), blob of detached slab, higher shear stress, shear affecting an uplifted lower mantle (Doglioni et al., 2009) and therefore they do not a priori represent the simple geometric prolongation of the shallow part of the slab.

When comparing the slab dip between 100 and 250 km of depth, and removing the subduction zones that are oblique with respect to the convergence direction, as Central America, the W-directed subduction zones show the larger (steeper) angles (Cruciani et al., 2005).

Moreover subduction zones, as a rule, juxtapose plates of different thickness and composition and this generates variation in the dip, e.g., a thicker plate with a stiff “vertical” margin will oblige the subducting slab to assume the shape of the overriding plate until it reaches its base, below the decoupling layer, at a depth of 100–150 km. The variability of the angle of obliquity of the subduction strike with respect to the convergence direction determines a further change in the dip of the slab, i.e., frontal subductions are steeper along the W-directed subduction zones than along E- or NE-directed ones. This is also evident from the foreland regional monocline that records the initial dip of the slab (Mariotti and Doglioni, 2000). In fact the dip is, on average, 6.1° along the W-directed subduction zones, while it is only 2.6° along the E- or NE-directed ones (Lenci and Doglioni, 2007).

In order to test the Lallemand et al. (2005) analysis, we re-computed the slab dip. In general, the W-directed subduction zones, when compared to E- or NE-directed slabs, show remarkable differences: (a) they are steeper, (b) they extend to greater depths and (c) they present a more coherent slab-related seismicity from the surface down to the 670 km discontinuity.

The dip of the slab perpendicular to the trench or strike of the subduction is given in Table 1 for W-directed and E- or NE-directed subduction zones. This measurement gives the maximum dip of the slab, regardless of the relative motion among upper and lower plates. In fact, the dip measured parallel to the convergence direction along a lateral ramp of a slab appears shallower. The measurements are based on geometries defined on the base of the seismicity (space distribution of hypocenters) alone, and not on images of inferred slabs based on tomography.

The selected subduction zones represent most of the world slabs. The analysis compares subduction polarity as a function of their strike with respect to the undulate mainstream of plate motion described by Crespi et al. (2007). The W-directed slabs are, on average, dipping 65.6°, whereas the E- or NE-directed slabs are dipping 27.1° (Fig. 4).

These results that are fully in agreement with Isacks and Barazangi (1977) who showed that western Pacific slabs are generally steeper than the eastern ones for most of their strike, are significantly different from those of Lallemand et al. (2005). The reasons for this difference could be the smearing effect that cannot be excluded in any mantle tomography (Raykova and Panza, 2006; Anderson, 2007b), and the arbitrary connection of the shallow slab seismicity with the deep isolated clusters along the E- or NE-directed subduction zones, or a combination of both. In fact, high-velocity bodies suggesting the presence of slabs in tomographic images often do not match slab seismicity, and the inference of slabs deeper than 250 km based on tomographic images is velocity model dependent and the color palette can be significantly misleading (e.g., Trampert et al., 2004; Anderson, 2006; 2007a,b).

There are at least three zones in the world where the same plate with similar composition subducts contemporaneously along two opposite subduction zones. These are 1) the central Mediterranean where the Ionian (oceanic)–Adriatic (continental) lithosphere subducts both westward beneath the Apennines, and NE-ward beneath the Dinarides–Hellenides; 2) the northern Australia where the passive continental margins subduct westward along the Banda arc and NE-ward along the Papua–New–Guinea subduction zone; and 3) the Molucche area where again a narrow segment of lithosphere is sinking along opposite subduction zones. In all these cases the W-directed slab-related seismicity, regardless of the age and composition of the subducting lithosphere, is steeper and reaches deeper than the E- or NE-directed one. Moreover there are no sub-vertical slabs beneath E-directed subduction zones, neither sub-horizontal slabs along W-directed subduction zones, whereas the contrary is observed (e.g., Mexico, Andes from almost 0° to 15°, and Mariannas, 80–90°).

The steeper E-directed slabs are seen along the Nicaragua and New Hebrides subduction zones, whereas the least steep W-directed slab is along Japan. These cases that are used as arguments against the existence of a global asymmetry, may, in fact be an exception to the global trend explained by regional conditions. The Japan subduction is

Table 1
Dip of the slab of the W- and E- or NE- directed subduction zones.

W-directed	Slab dip > 100 km	E- or NE-directed	Slab dip > 70 km	Deep cluster
Tohoku–Japan	35°	Nicaragua	50°	
Kuriles–Kamchatka	45°	Cascadia	18°	
Molucche 3°N	50°	Molucche 3°N	45°	
Aleutians 55°N/160°W	50°	New Hebrides	50°	yes
N–New Zealand 39°S	65°	Zagros	18°	
Banda	55°	Himalaya	15°	
Tonga	58°	Perù 10°S	10°	
Cotabago	63°	Perù–Bolivia 15°S	18°	yes
Mariannas 22°N	84°	Chile 22°S	21°	yes
Izu–Bonin 32°N	72°	Chile 24°S	21°	
Izu–Bonin 27°N	83°	Ecuador 3°S	20°	
Apennines	72°	Costarica	50°	
Sandwich	69°	Colombia 5°N	25°	
Barbados	68°	Hellenides	23°	
Mariannas 12°N	85°	Mexico	10°	
Mariannas 19°N	84°	Sumatra 100°E	32°	
Vrancea	78°	Sumatra 115°E	35°	yes
Average	65.6°	Average	27.1	

Data after Ammon et al. (2008); Sacks and Okada (1974); Isacks and Barazangi (1977); Barazangi and Isacks (1979); Pilger (1981); Vassiliou et al. (1984); McGeary et al. (1985); Jarrard (1986); Garfunkel et al. (1986); Oncescu and Trifu (1987); Bevis (1988); Cahill and Isacks (1992); Oncescu and Bonjer (1997); Engdahl et al. (1998); Gudmundsson and Sambridge (1998); Castle and Creager (1998); Gutscher et al. (1999); Chen et al. (2001); Karato et al. (2001); Engdahl and Villaseñor (2002); Rivera et al. (2002); Pardo et al. (2002); Billen et al. (2003); Hirth and Kohlstedt (2003); Das (2004); Lallemand et al. (2005); Milsom (2005); Syracuse and Abers (2006); Frepoli et al. (1996); Reyners et al. (2006); Billen and Hirth (2007); Vinnik et al. (2007); Chiarabba et al. (2008); Espurt et al. (2008); Pérez-Campos et al. (2008); and Scalera (2008).

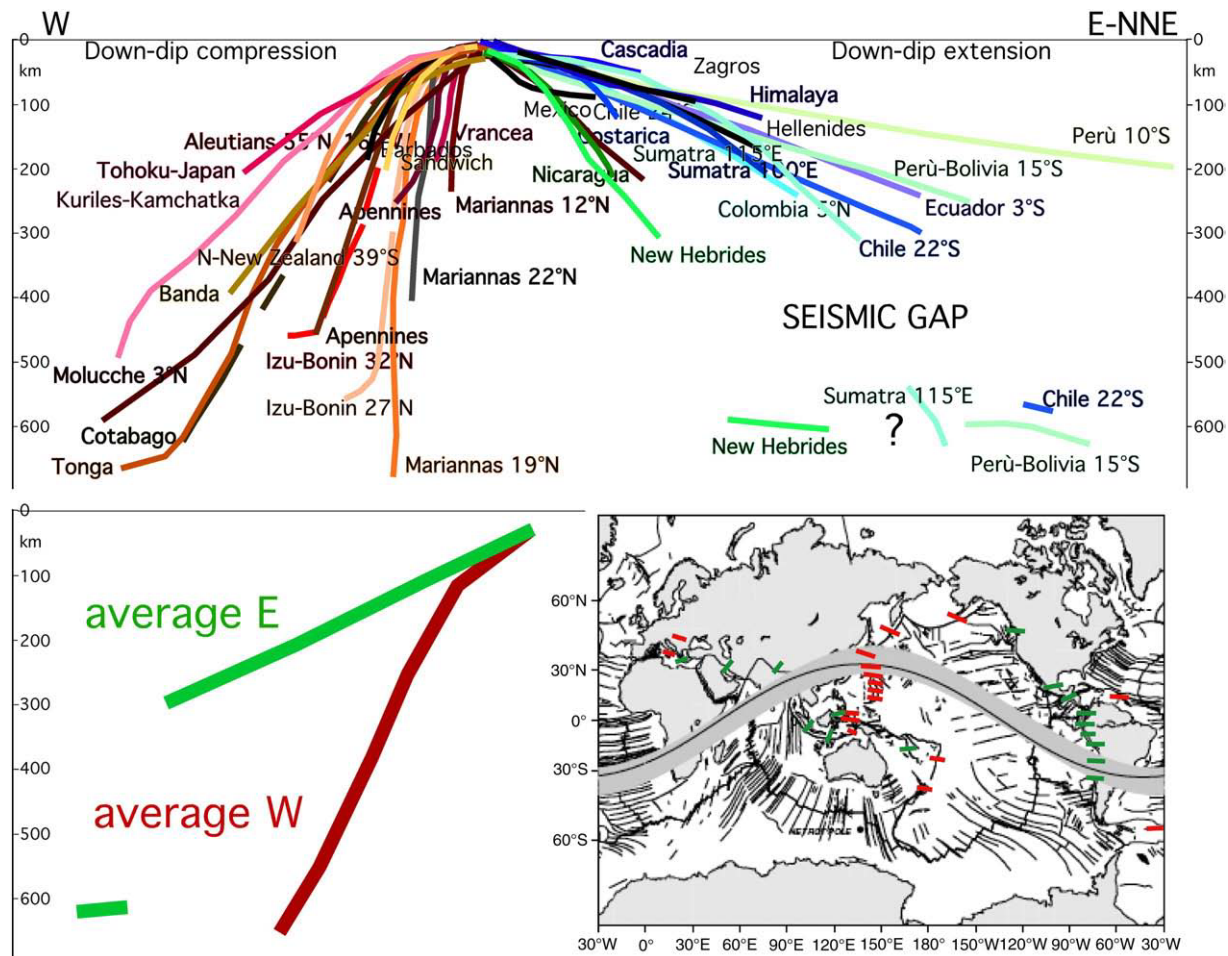


Fig. 4. Compilation of the slab dip measured along cross-sections perpendicular to the trench of most subduction zones. Each line represents the mean trace of the seismicity along every subduction. The asymmetry is also marked by the seismic gap between around 300–550 km occurring only along the E- or NE-directed subduction zones, that are, in general, shorter than the W-directed slabs. Some E- or NE-subduction zones present a deeper scattered cluster of hypocenters between 550–670 km which may be interpreted either as a detached fragment of the slab, or as a portion of lower mantle sucked from below, in the wake left by the slab in its anti-subduction (exhumation) motion (Doglioni et al., 2009). The dominant down-dip compression occurs in the W-directed intraslab seismicity, whereas down-dip extension prevails along the opposed E- or NE-directed slabs. The W-directed slabs are, on average, dipping 65.6°, whereas the average dip of the E- or NE-directed slabs, to the right, is 27.1° (see Table 1).

presently not following the standard kinematics of W-directed subduction zones where the subduction hinge migrates away from the upper plate; the hinge moves toward Eurasia and in fact the Japan Sea is shrinking. On the other hand, New Hebrides and Central America subduction zones have a relevant transpressional component (oblique subduction), which could contribute to the steepness of the slab. Australia is moving NNE-ward in the NNR (No-Net-Rotation reference frame, DeMets et al., 1990), and the NNW strike of the Vanuatu-New Hebrides trench implies that the subduction has a strong right lateral component (lateral-oblique subduction). Moving along the southern tip of the New Hebrides trench, where the subduction is in a frontal geometry, the slab is much less inclined ($<30^\circ$, Chatelain et al., 1993). The New Hebrides slab is quite short, with the typical seismic gap between 250–500 km. Similarly, the Central America slab has a left-lateral transpressive component, it is short, and becomes more flat along frontal segments of the subduction both to the south and to the north.

If the study of the slab dip is made based on mantle tomography images rather than on the space distribution of hypocenters a quite different picture can be drawn, e.g., the E-directed slabs appear longer and steeper. Thus this observation could be used to deny the asymmetry emerging from the analysis of the seismicity (the space distribution of hypocenters), but it must be kept in mind that the accuracy of the location of hypocenters clusters in the slabs (several tens of km) is comparable, if not much better, than the mantle

tomography resolution (few hundreds of km) (e.g. Vasco et al., 2003). This is due to the information content of the travel time data used in tomography experiments and to the dependence, on the initial reference velocity model, of the tomographic images that are routinely obtained by means of linear inversion. Assuming that the high-velocity bodies inferred from tomography are real, an alternative interpretation of these faster velocities is given by Doglioni et al. (2009). Relative to the mantle, W-directed subduction zones provide larger volumes of lithosphere re-entering into the mantle than the opposite E- or NE-directed slabs, which have a low sinking angle and could have a net motion in a direction opposed to the one of the subduction. This kinematics is consistent with an upward suction of the underlying mantle, with the upraising at shallower levels of mantle rocks that are thus naturally detected as a body with velocity higher than that of the surrounding medium. This generates on tomographic images an inclined column, usually much broader than a lithospheric slab, of faster mantle, which generates the phantom of a slab. In this hypothesis, along the E- or NE-directed subduction zones, beneath 300 km, the mantle tomography would not depict the real slabs, possibly being misleading in the study of the subduction zones.

The seismic coupling indicates the friction at the interface between upper and lower plates along subduction zones. This is lower along subduction zones where backarc spreading forms (Ruff and Kanamori, 1980). Backarc extension is typical of W-directed subduction zones where the subduction hinge migrates away relative to the upper plate

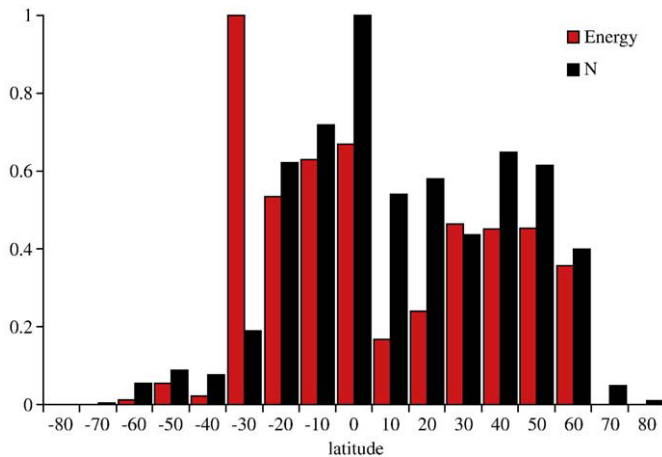


Fig. 5. Distribution of normalized N (number of earthquakes with $M_w \geq 7.0$) and E (elastic energy released by earthquakes with $M_w \geq 7.0$) grouped in 10° latitude bins, from the catalog – MGE7 global (earthquakes with $M_w \geq 7.0$ in the period 1900–2007). The outstanding energy release of the Chile earthquake (1960, $M_w = 9.5$) is well visible. Polar regions are silent whereas the seismic activity is maximum at low latitudes.

(Doglioni et al., 2007). High seismic coupling occurs where the subduction hinge converges relative to the upper plate, which is typical of E- or NE-directed subduction zones.

Another further asymmetry is the state of stress within slabs. W-directed subduction zones show predominantly down-dip compression of the intraslab seismicity, whereas E- or NE-directed slabs exhibit more frequently down-dip extension (Isacks and Molnar, 1971; Doglioni et al., 2007).

All these features have been interpreted as related to the “eastward” relative motion of the asthenosphere with respect to the lithosphere, which should determine not only different metamorphic and petrological evolutions (Peccerillo, 2005; Doglioni et al., 2007) but also different depths and behaviors of the basal decoupling planes. Moreover a relatively cooler mantle has been envisaged at the Earth’s equator (Bonatti et al., 1993), favoring the idea of a rotational component in mantle differentiation.

3. Latitudinal distribution of global seismicity

We have analyzed the global distribution of seismic events for magnitudes $M \geq 7.0$, which release about 90% of the elastic energy of plate tectonics, using the Centennial Catalog (CC) updated with the USGS/NEIC global catalog. We call this new catalog MGE7 global.

The CC is a global catalog which contains the locations and magnitudes of instrumentally recorded large earthquakes (Engdahl and Villaseñor, 2002). In this catalog that extends from 1900 to April 2002 all available magnitudes for each earthquake have been reduced to a common, reliable value. Thus completeness is practically ensured for magnitudes $M_w \geq 7.0$. The CC has been updated to September 2007 by adding all the events with $M_w \geq 7.0$ extracted from the USGS/NEIC global catalog. The MGE7 global contains 1719 events with $M_w \geq 7.0$ and the locations clearly delineate the plate margins and the deformation areas. Nevertheless, the seismicity is latitude dependent and decreases with increasing latitude. The distribution of the normalized frequency of the events in 10° bins shows that polar regions are not affected by seismic activity with $M_w \geq 7.0$, and that most of the events fall in the range $-10^\circ < \text{Lat} \leq 0^\circ$ N (Fig. 5). The normalized energy computed by the classical relationship (Kanamori, 1977) shows that more than 73% of the elastic energy is radiated in the range $-30^\circ < \text{Lat} \leq 30^\circ$ N. These patterns support a rotational and astronomical tuning of plate tectonics: at low latitudes, plates tend to move faster, transform faults are longer, seismic activity is globally higher, etc.

4. Length of the day (LOD) versus seismicity

Varga et al. (2005) have shown the existence of a relationship between the number of events occurring per year (N) and LOD time series: as LOD increases, N is higher and vice versa. Similar relation exists between the energy released globally by large events ($M_w \geq 7.0$) per year, and LOD. We have analyzed the time series of LOD, detrended from secular drift, N and $\log_{10}E$ considering a time span of more than a century (1900–2007). The LOD time series is composed by the yearly averaged time series of JPL (1832–1997) completed with the combined C04 solutions up to 2007, provided by the International Earth Rotation and Reference System Service (IERS) (Bizouard and Gambis, 2008). The N time series consists of the yearly number of events occurred from 1900 to September 2007, the $\log_{10}E$ time series is the \log_{10} of the global seismic energy yearly released. Since we are interested to identify long periods, the two time series are smoothed with a 5 yr moving average (a low-pass filter). To make an effective comparison, the two time series have been normalized. Fig. 6 shows the LOD, $\log_{10}E$ and N time series after the normalization.

The search for non-random processes in the normalized time series of LOD, $\log_{10}E$ and N is made, as a first step, by the Lomb normalized periodogram. LOD and N have significant peaks centered at 34 yr, corresponding respectively to normalized powers of 12.6 and 14.6, well beyond the value of 7.6, limit of the 95% level. The LOD and $\log_{10}E$ time series have significant periods at 51 yr, corresponding to normalized powers of 11.2 and 27.5 respectively.

The temporal interval common to the two time series is rather limited (102 yr), thus the detection of long periodicities is affected by a low resolution: the nearest peaks that can be really detected correspond to the frequency interval $f = 0.0294 \pm 0.0098 \text{ yr}^{-1}$ equivalent to the time interval of 25.5–51.0 yr. Therefore, we can conclude that the peaks identified in LOD, $\log_{10}E$ and N are significant but the time series are too short to detect with good resolution the real value of these periodicities.

The cross-correlation between the sequences has been computed in the frequency domain. The procedure is equivalent to the convolution with one of the two sequences reversed in time. At time lag 0, the cross-correlation between LOD and N is 0.79, and between LOD and $\log_{10}E$ is 0.81, both significant at the 95% confidence level. The magnitude squared spectral coherence is a positive normalized function of frequency and indicates how well one series corresponds to the other at each frequency. The spectral coherence of LOD and N approaches saturation at about 0.65 after about 20 yr; a higher level of coherence at low frequency is obtained between LOD and $\log_{10}E$, though it reaches the asymptotical value of about 0.78 after about 30 yr (Fig. 7).

It has been shown that seismicity is not able to significantly modify the LOD (Chao and Gross, 2005). Therefore the seismicity cannot be

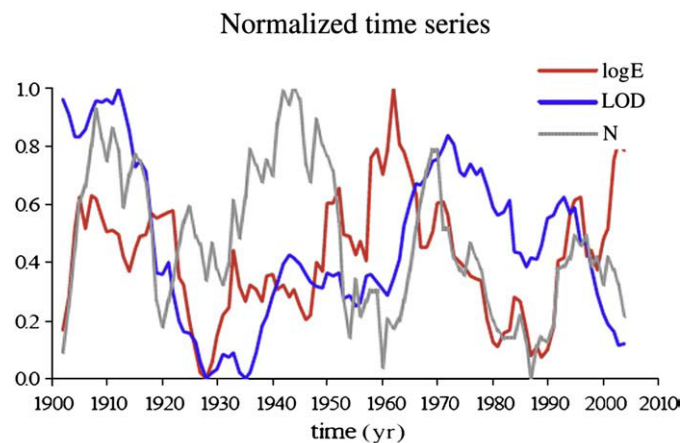


Fig. 6. Normalized time series of LOD (length of the day), N (number of earthquakes with $M_w \geq 7.0$), and $\log_{10}E$ (energy). The cross-correlation between LOD and N , and between LOD and $\log_{10}E$ is significant at 95% confidence level.

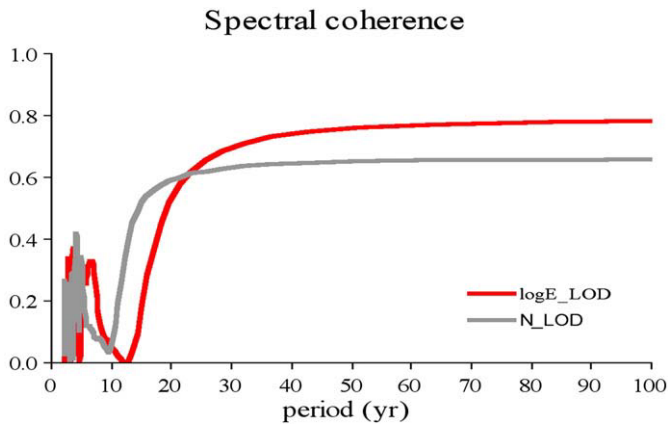


Fig. 7. Spectral coherence between LOD, N and LOD, $\log_{10}E$. The latter are more coherent at long periods than the first two. The saturation value of 0.65 is reached after 20 yr, when LOD and N are considered, while it reaches 0.78, after 30 yr, in the case of LOD and $\log_{10}E$.

responsible of the large and long-term LOD oscillations, and we argue that the process responsible for the LOD oscillation is the same as the one controlling the seismicity variation in time. Wang et al. (2000) have demonstrated a correlation between mounting stress and increase of the LOD along faults in China. The correlation appears most typically on decade time scales and seems to be direction-dependent.

The variability of the Earth's rotation vector relative to the body of the planet is caused by the gravitational torque exerted by the Moon, Sun and planets, displacements of matter in different parts of the planet and other possible excitation mechanisms. The solid Earth tides are deformations of the Earth that cause limited variations of the Earth's rotation vector and are not able to excite long period oscillations of LOD: the largest tidally induced LOD fluctuations are due to the fortnightly zonal tides, with amplitudes within 1 ms. Minor effects are due to monthly, semi-annual, and annual zonal tides (Yoder et al., 1981; Paquet et al., 1997), while the symmetric diurnal and semidiurnal tides cannot excite the LOD.

The secular linear decrease of the Earth rotation is mainly the consequence of a permanent phase lag in the deformation of the inelastic equatorial bulge due to the Moon attraction; its amplitude is estimated at 0.017 ms/yr (IERS Earth Orientation Center web site). To conserve the angular momentum of the system, the Earth's deceleration is mostly compensated by the enlarging of the Moon's orbit, at a rate of 38.2 ± 0.7 mm/yr (Dickey et al., 1994). The Earth spin has a variable rate now as in the past. The duration of day was about 19 h 2.5 Gyr ago, 21 h 0.5 Gyr ago, and it has been increasing during the last 500 Myr at a rate of about 1.79 ms/century (Denis et al., 2002).

The long-term variations of the Earth's angular velocity are mainly due to two different components with opposite effects: the tidal dissipation and the decrease of Earth oblateness, respectively acting to slow and to increase the Earth's angular velocity. The post-glacial rebound induces a net transfer of matter within the Earth toward higher latitudes, decreasing the Earth's moment of inertia and thereby decreasing LOD (Lambeck, 1980). There are shorter time scale variations of the LOD with wavelength of decades, or even seasonal and higher frequency oscillations (Jault et al., 1988; Kane and Trivedi, 1990; Marcus et al., 1998).

5. Solid Earth's energy budget and the plate tectonics expenditure

In plate tectonics it is assumed that the inertia and acceleration of the individual plates are nonexistent or negligible, and thus the plates are in dynamic equilibrium (Forsyth and Uyeda, 1975). At present, the solid Earth can be considered in energetic equilibrium: the energy sources that keep running its dynamical processes and the most

significant phenomena consumers of terrestrial energy resources are equivalent in magnitude (see the Appendix). Thus it is natural to assume that the balance is in quasi equilibrium, i.e. there is no statistically meaningful difference between the total of income and expenditure energy rates. This circumstance allows for relatively small energy sources to influence global tectonic processes and we think the tidal despinning is able to influence plate tectonics through the westward lithospheric drift (Bostrom, 1971; Knopoff and Leeds, 1972). Small perturbations in the velocity of rotation trigger the release of a large amount of energy and seismicity (Press and Briggs, 1975). The energy rate necessary to move the Earth's shields, i.e. to move the thicker lithosphere relative to the underlying poorly developed low-velocity channel (as in the Baltic area), has been estimated at about $4 \cdot 10^{18}$ J/yr (Knopoff, 1972). Similar value is found by considering the energy of formation of tectonic dislocations that can be estimated as the consume of energy rate \dot{E} necessary for lateral displacement of the lithosphere plates relative to the viscous mantle. Thus, it can be written as (Maslov, 1991).

$$\dot{E} = \chi \cdot \omega^2 \cdot \frac{a^4 \cdot \pi^2}{4 \cdot h} = \chi \cdot v^2 \cdot \frac{a^2 \cdot \pi^2}{4 \cdot h} = \chi \cdot v^2 \cdot \frac{D^2}{h}$$

One classical value of mantle viscosity is $\chi = 10^{22}$ Poise (1P = 0.1 Pa s), the plate angular (lateral) speed $\omega = 1.7 \text{ }^\circ/\text{yr} \cdot 10^{-6}$ ($v = 2$ cm/yr), $a = 6.371 \cdot 10^8$ cm the mean Earth's radius and the thickness of the crust $h = 100$ km one gets $\dot{E} = 1.27 \cdot 10^{19}$ J/yr. In the above equation $D = \pi \cdot a / 2$ ($D = 1 \cdot 10^9$ cm) serves as horizontal scale of the plates.

If we consider the whole lithosphere this value has to be multiplied for $16/\pi$ obtaining $\dot{E} = 6.5 \cdot 10^{19}$ J/yr. Recent papers show a model of post-seismic relaxation indicating viscosity values of 10^{18} Poise (Aoudia et al., 2007; Melini et al., 2008). Consequently, the power needed to move the lithosphere could be significantly lowered, possibly to $\dot{E} = 6.5 \cdot 10^{15}$ J/yr.

The tidal friction in the Earth–Moon system can be determined on the basis of the temporal variation of the Earth's rotational energy plus the Moon orbital's energy

$$E_T = \frac{1}{2} C \omega^2 + \frac{1}{2} a_m^2 n_m^2 \cdot \left(\frac{M \cdot M_m}{M + M_m} \right) - G \frac{M \cdot M_m}{a_m}$$

where C , ω and M are the polar moment of inertia, the angular speed and the mass of the Earth, and a_m , n_m and M_m are the Earth–Moon distance, the Moon's orbital speed and the mass of the Moon, respectively, while G stands for the gravitational constant. Using Kepler's third law and conservation of momentum in the Earth–Moon system, $\dot{E} = C = (\omega - n_m) \dot{\omega}$; introducing the parameter's values provided by the IERS, we obtain $\dot{E} = 1.2 \cdot 10^{20}$ J/yr. Most of this dissipation occurs in the oceans and shallow seas and only a limited part in the mantle. According to Ray (2001) the tidal dissipation in the mantle amounts maximum to $0.42 \cdot 10^{19}$ J/yr, whereas the total oceanic and shallow seas dissipation is about $0.75 \cdot 10^{20}$ J/yr (Egbert and Ray, 2000). Therefore the residual available power, about $0.4 \cdot 10^{20}$ J/yr is larger than the one required to move the lithosphere with respect to the mantle, and we think that the Earth's rotation plays a key role in the generation of the relative shear.

6. The decoupling in the upper asthenosphere

The decoupling at the base of the lithosphere is suggested by a number of independent evidences, namely 1) the motion of the Pacific plate relative to the mantle source of the Hawaii volcanic track, as well as similar seamounts trails, needs a decoupling zone between lithosphere and the magmatic source; 2) the kinematic of plates indicates a migration of plate boundaries relative to each other and relative to the mantle (e.g., Garfunkel et al., 1986); 3) the shear wave splitting analysis points out for a shear between the lithosphere and the mantle,

concentrated in the asthenosphere, where olivine crystals tend to align along the direction of motion of plates relative to the mantle (Gung et al., 2003; Debayle et al., 2005); 4) the notion of the net rotation or westward drift of the lithosphere computed in the hotspot reference frame (Gripp and Gordon, 2002), and supported by the asymmetry of tectonic features, requires a generalized decoupling between the lithosphere and the mantle, regardless of its nature (Doglioni, 1993); 5) the top of the asthenosphere (100–220 km) is marked by a pronounced decrease in velocity (the Low Velocity Zone, LVZ) of both P and S seismic waves, pointing for the occurrence of some melt (Panza, 1980); 6) most of the Earth's magmatism forms in the upper asthenosphere (e.g., Foulger and Jurdy, 2007), and the partial melting decreases the viscosity; and 7) the faster plate relative to the mantle has the lowest measured viscosity values (5×10^{17} Pa s, Pollitz et al., 1998).

The amount of decoupling in the asthenosphere is function of the viscosity of the layer. Moreover, the viscosity of the asthenosphere computed on the time scale of post-glacial rebound (10 ka) can be significantly different from the one related to long lasting processes (10 Ma). The viscosity quantifies the resistance of a fluid to flow, and it is the ratio between the shear stress and the strain rate. Some materials have a viscosity that depends on the time scale of an applied shear stress. The time scale of tidal drag can be considered as infinite. Studies of the mantle's mechanical properties during the last decades have repeatedly pointed out the non linear rheology of the mantle (e.g., Caputo, 1986; Kornig and Muller, 1989; Ranalli, 1995), which usually implies that viscosity in the asthenosphere decreases as the shear stress raises. The viscosity of the mantle based on the post-glacial rebound computation has four main limitations to our purpose: 1) it gives values at a much shorter time scale than the one of plate tectonic processes; 2) the viscosity is averaged on the mantle section loaded and unloaded by the ice cap, e.g., 2000 km, about 10 times thicker than the upper asthenosphere that may locally have much lower viscosity; 3) the viscosity is inferred by vertically loading and unloading the mantle, being 1 to 3 orders of magnitude higher than the viscosity measured under horizontal shear; and 4) a 50–100 km thick layer with low viscosity remains invisible to post-glacial rebound modeling.

Jordan (1974) recognized that the tidal despinning is supplying a relevant amount of energy sufficient to move plates, but he argued that the viscosity of the asthenosphere is too high in order to allow a decoupling of the overlying lithosphere induced by the Earth's rotation (Ranalli, 2000). However new evidences support the presence of an ultra-low seismic velocity at the top of the asthenosphere (Rychert et al., 2005), which might correspond to the presence, in the asthenospheric LVZ, of a layer with much lower viscosity than so far expected (Rychert et al., 2005; Aoudia et al., 2007). A justification for the existence of an ultra-thin viscosity anisotropy zone in the asthenosphere is supplied by Marone and Romanowicz (2007), even though so far limited to whole North America. Their Fig. 4c clearly shows the necessity of a thin decoupling zone at a depth of about 200 km where there is an abrupt shift of about 90° of the fast axis direction. Petrological and laboratory experiments also point for very low viscosity in the asthenosphere, particularly when intra-crystal pockets of melt occur (Hirth and Kohlstedt, 1995; Holtzman et al., 2003; Dingwell et al., 2004; Liebske et al., 2005). Water content in the asthenosphere can drastically lower its viscosity to 10^{15} Pa s (Korenaga and Karato, 2008). Moreover, the viscosity in the asthenospheric LVZ can be orders of magnitude lower when measured under horizontal shear with respect to the viscosity computed by vertical unloading due to post-glacial rebound (Scoppola et al., 2006).

It is important to remember that a thin ultra-low viscosity layer is invisible to post-glacial rebound viscosity computation due to the channel flow effect (Cathles, 1975) or to the geoid variation (Marquart et al., 2005). Therefore the occurrence of such a layer cannot be excluded a priori. The larger decrease in velocity of Vs than Vp in the low-velocity layer points for a significant amount of melt in the upper

asthenosphere, accordingly to the fact that the geotherm is warmer than the solidus at 150–200 km depth. Electromagnetic studies seem to support the presence of an intra-asthenosphere layer with larger amount of fluids (Heinson, 1999) that would drop the LVZ viscosity.

Jin et al. (1994) have shown how the intra-crystalline melt in the asthenospheric peridotites under shear can generate a viscosity of about 10^{12} Pa s (Stevenson, 1994), a value compatible with the plate tectonics driven by the Earth's rotation (Scoppola et al., 2006).

Therefore the presence of an ultra-low viscosity layer in the upper asthenosphere (Fig. 1) can be considered as a possibility with the present available techniques of mantle sampling and laboratory experiment.

7. Model

The Earth system (solid Earth + hydrosphere + atmosphere) has an effective viscoelasticity which reacts with some delay with respect to the Earth and Moon alignment. The Earth would tend to move backward along this alignment (Fig. 8). The about $2\text{--}3^\circ$ tidal lag angle between the tidal bulge and the gravitational alignment between the Earth and the Moon (e.g., Touma and Wisdom, 1994) determines a permanent torque toward the “west”, opposite to the E-ward rotation of the planet. This torque is considered responsible for the secular deceleration of the Earth, and acts directly on the lithosphere.

In our model, the visco-elastic lithosphere (say 100 km thick) is dragged “westward” by the tidal torque, above a decoupling zone (50–100 km thick) with visco-plastic behavior, corresponding to the LVZ in the asthenosphere. The LVZ, where the mantle partly melts because the geotherm is higher than the mantle solidus, should correspond to a drastic decrease in viscosity of the upper asthenosphere, allowing the tidal torque to focus the dissipation of its energy in this layer (Fig. 9). It has to be noted that the mainstream of plate motion described by Crespi et al. (2007) has an angle of about 30° with respect to the equator, close to the revolution plane of the Moon about the Earth (28°), although this overlap is intermittent.

The solid Earth tide accompanies this translation provoking a semidiurnal oscillation of the lithosphere. The period 12 h25'

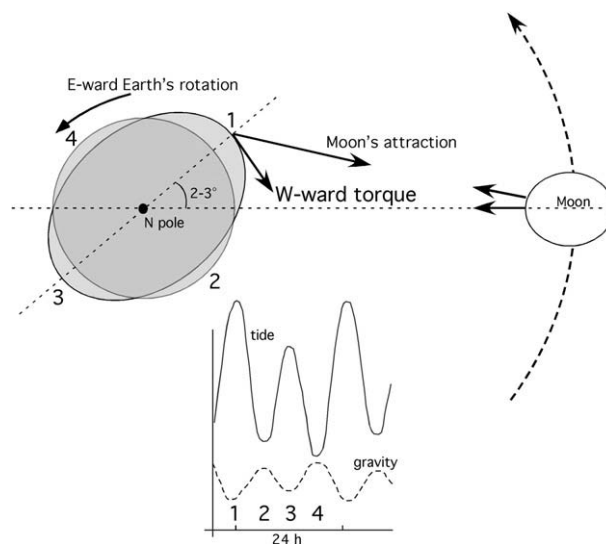


Fig. 8. Cartoon showing the Earth's bulge deviation (delay) from the (gravitational) Earth–Moon alignment of about $2\text{--}3^\circ$ due to the visco-elastic nature of the Earth. This distribution of the mass tends to pull the planet along the gravitational alignment, acting permanently toward the “west”, on the Moon's revolution plane. Since it acts in versus opposed to the E-ward rotation of the planet, this torque is considered responsible for the slow Earth's despinning. The torque can push the lithosphere horizontally, westward relative to the underlying mantle: tides generate waves that swing the lithosphere horizontally and vertically, and are accompanied by gravity variations of opposed sign. Therefore the lithosphere undergoes a permanent, isoriated oscillation.

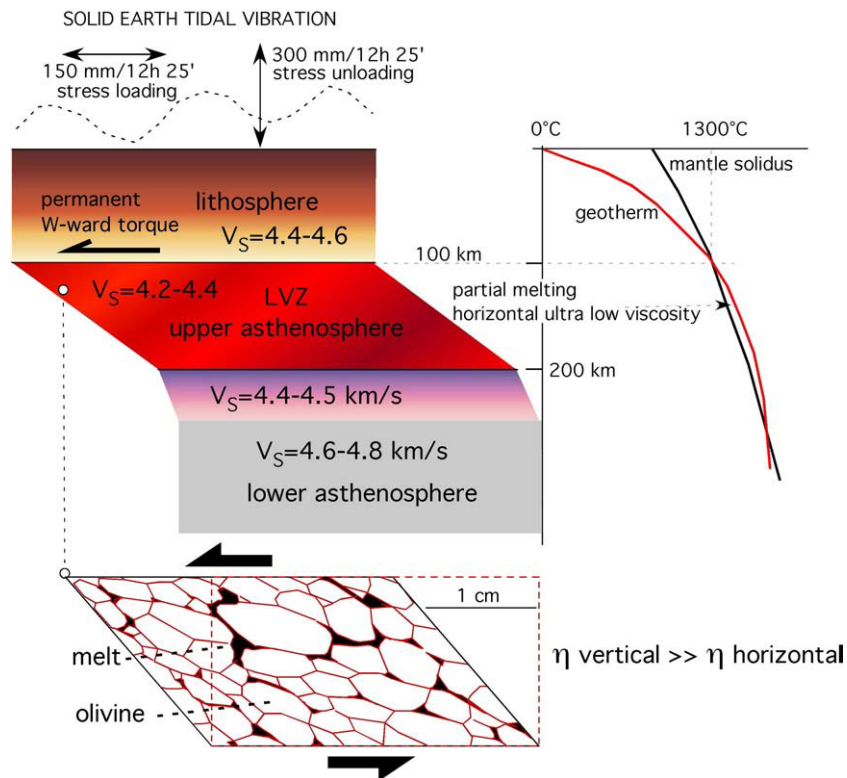


Fig. 9. Is focused in the asthenosphere, where the geotherm is above the temperature of mantle solidus, and small pockets of melt can induce a strong decrease of the viscosity in the upper part of the asthenosphere. The viscosity in this layer, the Low Velocity Zone of the asthenosphere, can be much lower than the present-day estimates of the asthenosphere viscosity based on the post-glacial rebound, because the horizontal viscosity under shear can be several orders of magnitude lower than the vertical viscosity computed averaging the whole asthenosphere. This should be the basic decoupling zone for plate tectonics, where the lithosphere moves relative to the underlying mantle. Tidal waves are too small to generate plate tectonics. However, their horizontal isoriented movement, might determine a fundamental consequence. The lithosphere, being swung horizontally by the solid tide of say 150 mm/semidiurnal, may, under a permanent torque, retain a small but permanent strain (e.g., a shift of 0.1 mm/semidiurnal). At the end of the year this slow restless deformation amounts to a cumulative effect of several centimeters which is consistent with the observed plate motion and thus could be what we consider the net rotation of the lithosphere.

corresponds to the mean semidiurnal lunar wave M_2 , which is responsible first of all for the generation of tidal bulge; the solid Earth tides have a well-known vertical oscillation of 300–400 mm/12 h25', but they also have a relevant 150–200 mm/12 h25' horizontal swinging. Under a permanent torque, this oscillation may induce a tiny strain in the upper asthenosphere, say 0.1–0.2 mm. The cumulative effect of this small horizontal motion, which repeats twice a day, may well reach several centimeters (7–14) per year necessary to guarantee a lithosphere plate motion, at least partly decoupled from the deeper mantle, i.e., the net rotation or so-called W-ward drift of the lithosphere relative to the mantle (e.g., Crespi et al., 2007). In other words the horizontal shear determined by the persisting westward torque acting on an asthenosphere that undergoes the mechanical fatigue exerted by the semidiurnal tidal oscillation, might allow the relative motion of the overlying lithosphere. The advantage of this mechanism is to act contemporaneously all over the lithosphere.

A statistically significant correlation has been shown between seismicity ($M \geq 5.5$ global shallow thrust earthquakes) and higher peak tidal stresses at continent–ocean margins, where there is a large ocean-loading component of tidal stress (Ray, 2001). However, compressive earthquakes occur more frequently during the high tide (Cochran et al., 2004) whereas extensional earthquakes are more frequent during low tides (Wilcock, 2001). In compressional tectonic settings the vertical load is expressed by σ_3 , whereas it is given by σ_1 in extensional tectonic settings. During a high tide (both solid and fluid) we could expect a thicker section of rocks and water and therefore an increase of the lithostatic load. However, during the high tide, the gravity is at the minimum, opposite to the sign of the tide. Therefore, the lithostatic load (ρgz , where ρ is density, g , gravity, and z , thickness) becomes smaller during the high tide, and larger during

the low tide. This oscillating wave determines a decrease of σ_3 during the high tide, and an increase of σ_1 during the low tide. In the first case the Mohr circle enlarges to the left, while in the second case it enlarges to the right. Both opposite cases facilitate rupture in compressional and extensional settings respectively (Fig. 10).

In this view, the oscillating horizontal component of the tides load and pump the tectonic system, drop by drop, slowly but steadily, whereas the vertical component of the tides might be the unloading mechanism when enough energy has accumulated along fault zones. As an example, during the recent Apennines L'Aquila earthquake sequence (April 6, 2009), the main event ($M_w = 6.3$, extensional focal mechanism, NEIC) occurred very near to a gravity maximum (low solid tide), thus suggesting that the larger the lithostatic load, the larger is σ_1 and the activation of extensional stresses.

Since the lithosphere has been documented to be in a critical state, small variations of the lithostatic load even of few Pascal may trigger the rupture or the slow viscous flow of rocks (e.g., Twiss and Moores, 1992).

8. Discussion and conclusions

In this paper we describe in detail the asymmetry between W-directed and E- or NE-directed subduction zones, both in terms of morphology (Fig. 3), geology, and geophysical signatures (Fig. 4). The distribution in space and time of global seismicity ($M_w \geq 7$) is latitude dependent (Fig. 5), being very low in the polar regions. Moreover, the time series of LOD, $\log_{10}E$ and N (Fig. 6) have significant correlation and spectral coherence, particularly for periodicities longer than 25.5 yr (Fig. 7). The LOD decrease corresponds to an increase of the Earth's oblateness and to a polhody amplitude decrease (Lambeck, 1980; Bizouard and Gambis, 2008). Accordingly modulated are the occurrence of large seismic events and

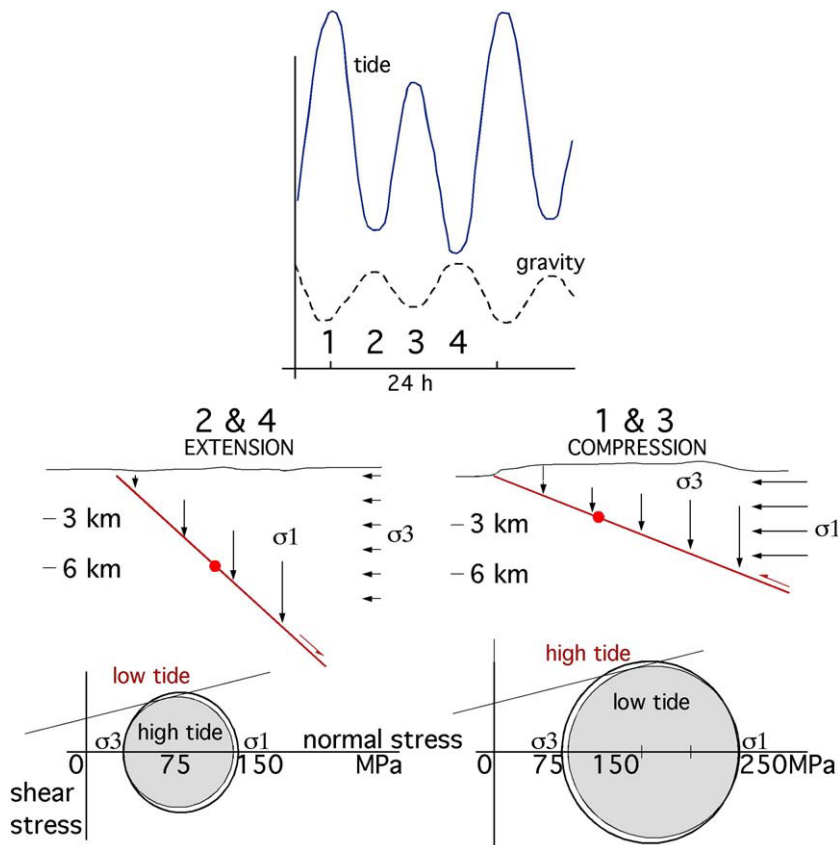


Fig. 10. During their passage, tidal waves determine very small variations of gravity. However these slight variations of the lithostatic load, acting on a lithosphere, which is slowly but persistently pumped westward, could determine the increase or decrease of σ_1 in extensional environments, or σ_3 in compressional tectonic settings. Therefore the same variation of the lithostatic load acts in an opposite way in the two different tectonic settings. In this model, the horizontal component of the solid Earth tide slowly accumulates the stress, whereas the vertical component could allow the downloading of the stress as a function of the tectonic setting and the orientation of the faults relative to the tidal waves.

the release of seismic energy: as the Earth slows down (increase of LOD) the seismicity (either E or N) increases and vice versa. We speculate that similar periodicities should affect also GPS velocities when sufficient time span of measurements will be covered, i.e., plates should move with similar periodicities, due to oscillating tidal torques and Earth's oblateness acting on the lithosphere.

The up and down of the solid Earth tides are too small to drive plates (e.g., Ray et al., 2001). However, the horizontal permanent torque exerted by the misalignment of the tidal bulge and the Earth–Moon gravitational trajectory rather provides a relevant amount of energy. We have reviewed the gross energy budget of the Earth, and the rotational-despinning energy dissipation can be considered sufficient to contribute significantly in moving plates, particularly if an ultra-low viscosity layer is present at the top of the asthenosphere, allowing the relative westward decoupling of the lithosphere.

The lithosphere and the underlying mantle represent a self-organized system in a critical state – SOC system (Stern, 2002) – open to external perturbations; plate tectonics is an example of a self-organizing complex system of hierarchical blocks in a critical state (Prigogine and Stengers, 1984). The Gutenberg–Richter law shows that large magnitude earthquakes are very rare events (Stein and Wysession, 2003), thus the energy released by one big earthquake seems to deplete temporally the energy budget of plate tectonics, i.e. a slab interacting with the surrounding mantle is not an isolated system, but it participates to a global expenditure of the stored energy.

Plate tectonics is an Earth's scale phenomenology, and the energy source for its activation is not concentrated in limited zones (e.g., subduction zones), but it acts contemporaneously all over the whole Earth's lithosphere, like the Earth's rotation. Romashkova (2009) has recently shown how the planet seismicity indicates that the Earth's lithosphere can be considered as a single whole. Only the global

seismicity follows the Gutenberg–Richter law, while this simple SOC relation does not hold when considering smaller portions of the Earth (Molchan et al., 1997). All these evidences and models are in favor, even if not conclusive, of a significant contribution to plate tectonics by the Earth's rotation.

Our model supports an origin of plate tectonics in which the classic mantle convection is complemented and polarized by the steady-state torque provided by the tidal bulge misalignment. The horizontal component of the Earth's tide pumps the system; the vertical component of the tides excites gravity oscillations, which locally load and unload the tectonic features (Fig. 11). Low solid tide (larger gravity) favors extensional tectonics, whereas high solid tide (lower gravity) triggers compressional tectonics.

The differential velocity among plates would be controlled by the viscosity-related variable decoupling at the base of the lithosphere,

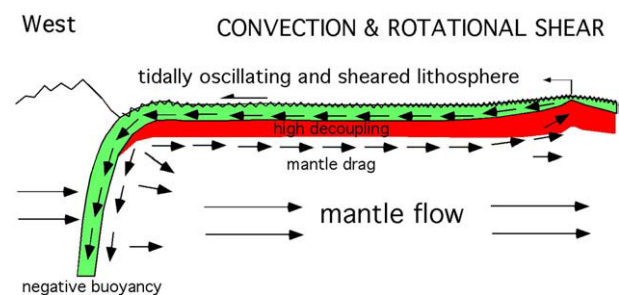


Fig. 11. Schematic flow patterns describing the coexistence of Earth's convection and the rotational shear. In this model, the cooling of the Earth, enhancing mantle convection, is added by the shear associated to the horizontal component of the solid Earth tide, thus triggering the westward drift of the lithosphere.

combined with other forcing mechanisms of mantle convection such as mantle drag and slab pull. Numerical and analogue modeling should further test this model.

Acknowledgements

P. Varga acknowledges the support of the Hungarian Scientific Research Fund OTKA in the framework of project K 60394 (“Interaction of Earth rotation and geodynamical processes”). We are grateful to all the persons involved in the IERS-EOP database maintenance (<http://hpiers.obspm.fr/eop-pc/>). Discussions with E. Bonatti, E. Carminati, M. Cuffaro, R. Devoti and F. Innocenti were very stimulating. We thank L. Knopoff for helpful comments on an earlier version of this article. C. Bizouard and an anonymous referee reviewed the article.

Appendix A

Earth's energy budget and the plate tectonics expenditure

Table 2 shows the energy sources that keep running the dynamical processes of the Earth and the phenomena that are the most significant consumers of terrestrial energy resources.

According to Iriyama (1977), the most important sources of energy income rate are the accretion \dot{E}_A , the core formation (differentiation) \dot{E}_C , the radioactive decay (radiogenic heat production) \dot{E}_R and the tidal friction \dot{E}_T . The main components of the energy expenditure rate of the Earth's planetary energy budget are represented by the heat flow \dot{E}_{HF} and the global tectonic moment rate \dot{E}_{TM} , following the global estimation of Kreemer et al. (2002). The annual rate values here reported are the results of a compilation of the estimates available in the literature, here briefly discussed.

The real errors of the estimates reported in Table 2 cannot be determined so that we prefer to discuss their order of magnitude. Thus it is natural to assume that the balance is in quasi equilibrium, i.e. there is no statistically meaningful difference between the total of energy rate income and energy rate expenditure.

There are several attempts of estimation of solid Earth's energy rates; consequently we consider useful to report here the minimum and maximum values found in literature.

Energy income rate

Accretion

The birth and infancy of the Earth was a time of gravitational accumulation and profound differentiation. The total of our knowledge indicates that, in all probability, these events were comparatively rapid and took place very early and simultaneously with the formation of the Earth itself. The time span of accretion and differentiation (core formation) should be between 100 thousand to hundred million years (Monin, 1978; Walter and Trønes, 2004).

The energetics of the gravitational accumulation process has two different scenarios:

- the kinetic energy of the large number of small particles approaching the proto-planet is used for heating.

- the kinetic energy of falling bodies is used up for erosion of the globe (cratering and ejection of fragments of rocks from the planet).

The accretion energy rates \dot{E}_A given by different authors, to characterize the accretion process, show a relatively significant scatter that depends upon the kind of assumptions made, namely:

- $1.9 \cdot 10^{21}$ J/yr (Sasaki and Nakazawa, 1986)
- $4.9 \cdot 10^{21}$ J/yr (Janle and Meissner, 1986)
- $4.9 \cdot 10^{21}$ J/yr (Verhoogen, 1980)
- $5.6 \cdot 10^{21}$ J/yr (Iriyama, 1977)

thus

$$\begin{aligned}\dot{E}_A \text{ min} &= 1.9 \cdot 10^{21} \text{ J/yr (Sasaki and Nakazawa, 1986)} \\ \dot{E}_A \text{ max} &= 5.6 \cdot 10^{21} \text{ J/yr (Iriyama, 1977)}\end{aligned}$$

Core formation

The range of core formation energy rates \dot{E}_C presented in different contributions is relatively small due to the use of more or less similar theoretical models:

- $3.2 \cdot 10^{21}$ J/yr (Flasar and Birch, 1973)
- $3.3 \cdot 10^{21}$ J/yr (Iriyama, 1977)
- $3.5 \cdot 10^{21}$ J/yr (Monin, 1978)
- $3.6 \cdot 10^{21}$ J/yr (Birch, 1965)

thus

$$\begin{aligned}\dot{E}_C \text{ min} &= 3.2 \cdot 10^{21} \text{ J/yr (Flasar and Birch, 1973)} \\ \dot{E}_C \text{ max} &= 3.6 \cdot 10^{21} \text{ J/yr (Birch, 1965)}.\end{aligned}$$

Radioactive decay

In the earliest stage of the Earth's history (4 billion years BP) the radiogenic heat production was about five times higher than at the Present Epoch (Rybach, 1976). Short-lived isotopes with half-lives of 10^5 – 10^7 yr, or even much shorter, may have had sufficient effect to melt the central parts of the forming proto-planet. Over the 4.6 Eon (Eon = 10^9 yr) lifetime of the Earth, four long-life isotopes ^{238}U , ^{235}U , ^{232}Th and ^{40}K gave the most important contribution to the radiogenic heat production. The amount of radioactive heat in the crust is 8 TW, in the mantle 23 TW, while in the core it is about 9 TW (Anderson, 1989). More recently Lay et al. (2008) slightly increase these values to a total of 46 ± 3 TW, although a debate on the topic is still alive; for example Hofmeister and Criss (2005) suggest a lower value (31 ± 1 TW). The radioactive annual rates \dot{E}_R published in different scientific contributions are:

- $2.1 \cdot 10^{20}$ – $2.1 \cdot 10^{21}$ J/yr (Bott, 1982)
- $1.3 \cdot 10^{21}$ J/yr (Anderson, 1989)
- $2.1 \cdot 10^{21}$ J/yr (Iriyama, 1977)

thus

$$\begin{aligned}\dot{E}_R \text{ min} &= 0.2 \cdot 10^{21} \text{ J/yr (Bott, 1982)} \\ \dot{E}_R \text{ max} &= 2.1 \cdot 10^{21} \text{ J/yr (Iriyama, 1977)}.\end{aligned}$$

Tidal friction

The tidal friction energy rate \dot{E}_T is $(0.04$ – $0.12) \cdot 10^{21}$ J/yr. The value of the despinning rate was five time smaller during Archean and Proterozoic than during the last 570 Ma (Phanerozoic) (Varga, 2006).

Thus,

$$\begin{aligned}\dot{E}_T \text{ min} &= 0.04 \cdot 10^{21} \text{ J/yr (Zschau, 1986)} \\ \dot{E}_T \text{ max} &= 0.11 \cdot 10^{21} \text{ J/yr (Varga, 2006)}\end{aligned}$$

Table 2

Energy budgets of the solid Earth.

Energy income (J/yr) $\times 10^{21}$		Energy expenditure (J/yr) $\times 10^{21}$	
Accretion \dot{E}_A	1.9–5.5	Heat flow \dot{E}_{HF}	1.4–1.5
Core formation \dot{E}_C	3.2–3.6		
Radioactive decay \dot{E}_R	0.2–2.1	Tectonic moment rate \dot{E}_{TM}	5.7–7.6
Tidal friction \dot{E}_T	0.04–0.1		
Total energy income	5–11	Total energy expenditure	7–9

Total energy income rate $\dot{E}_{IN} = (5 \div 11) \cdot 10^{21}$ J/yr. Then, the average value is

$$\dot{E}_{IN}^{Av} = (8 \pm 3) \cdot 10^{21} \text{ J/yr}$$

Energy expenditure

Heat flow

$$\dot{E}_{HF} \text{ min} = 1.4 \cdot 10^{21} \text{ J/yr (Turcotte and Schubert, 2002; Lowrie, 2007).}$$

$$\dot{E}_{HF} \text{ max} = 1.5 \cdot 10^{21} \text{ J/yr (Lay et al., 2008).}$$

Tectonic moment rate

Numerically, most of the energy expenditure goes into the global tectonic momentum \dot{E}_{TM} and this shows that most of the energy loss is related to plate tectonic activities. The tectonic moment rate estimated by Kreemer et al. (2002) is $7.0 \cdot 10^{21}$ and is considered by the authors as a minimum value because it is estimated during a period of low seismic activity and on a short time span. Effectively, the tectonic moment rate strongly depends on the level of seismicity. Consequently we have recomputed this rate on our catalog (see the main manuscript) and applying the geometrical mean first on the same time span of Kreemer et al. (2002), obtaining the minimum value; then on the whole catalog, obtaining the maximum value.

$$\dot{E}_{TM} \text{ max} = 5.7 \cdot 10^{21} \text{ J/yr}$$

$$\dot{E}_{TM} \text{ min} = 7.6 \cdot 10^{21} \text{ J/yr}$$

Total energy expenditure $\dot{E}_{OUT} = (7 \div 9) \cdot 10^{21}$ J/yr. Then, the average value is

$$\dot{E}_{OUT}^{Av} = (8 \pm 3) \cdot 10^{21} \text{ J/yr}$$

Energy expenditure-income $\Delta \dot{E} = 0$ J/yr.

The balance is again in quasi equilibrium, i.e., there is no statistically meaningful difference between the total of energy rate income and expenditure.

References

Altamimi, Z., Collilieux, X., LeGrand, J., Garayt, B., Boucher, C., 2007. ITRF2005. A new release of the International Terrestrial Reference Frame based on time series of station positions and Earth Orientation Parameters. *J. Geophys. Res.* 112, B09401. doi:10.1029/2007JB004949.

Ammon, C.J., Kanamori, H., Lay, T., 2008. A great earthquake doublet and seismic stress transfer cycle in the central Kuril islands. *Nature* 451. doi:10.1038/nature06521.

Anderson, D.L., 1989. Theory of the Earth. In Blackwell, pp. 1–366.

Anderson, D.L., 2006. Speculations on the nature and cause of mantle heterogeneity. *Tectonophysics* 416, 7–22.

Anderson, D.L., 2007a. New Theory of the Earth. Cambridge University Press. ISBN 978-0-521-84959-3, 0-521-84959-4.

Anderson, D.L., 2007b. Is There Convincing Tomographic Evidence for Whole Mantle Convection? <http://www.mantleplumes.org/TomographyProblems.html>.

Aoudia, A., Ismail-Zadeh, A.T., Romanelli, F., 2007. Buoyancy-driven deformation and contemporary tectonic stress in the lithosphere beneath Central Italy. *Terra Nova* 19, 490–495.

Baranzangi, M., Isacks, B.L., 1979. Subduction of the Nazca plate beneath Peru: evidence from spatial distribution of earthquakes. *Geophys. J. R. Astron. Soc.* 57, 537–555.

Bevis, M., 1988. Seismic slip and down-dip strain rates in Wadati–Benioff Zones. *Science* 240, 1317–1319.

Billen, M.I., Hirth, G., 2007. Rheologic controls on slab dynamics. *Geochem. Geophys. Geosyst.* 8, Q08012. doi:10.1029/2007GC001597.

Billen, M.I., Gurnis, M., Simons, M., 2003. Multiscale dynamic models of the Tonga–Kermadec subduction zone. *Geophys. J. Int.* 153, 359–388.

Birch, F., 1965. Energetics of core formation. *J. Geophys. Res.* 69, 4377–4388.

Bizouard, C., Gambis, D., 2008. The Combined Solution C04 for Earth Orientation Parameters, Recent Improvements. Springer Verlag series.

Bonatti, E., Seyler, M., Sushevskay, N., 1993. A cold suboceanic mantle belt at the Earth's equator. *Science* 261 (5119), 315–320. doi:10.1126/science.261.5119.315.

Bostrom, R.C., 1971. Westward displacement of the lithosphere. *Nature* 234, 356–358.

Bostrom, R.C., 2000. Tectonic Consequences of the Earth's Rotation. In Oxford University Press, pp. 1–266.

Bott, M.P.H., 1982. The Interior of the Earth: Its Structure, Construction and Evolution. E. Arnold Publ. Ltd.

Cahill, T., Isacks, B.L., 1992. Seismicity and shape of the subducted Nazca plate. *J. Geophys. Res.* 97, 17,503–17,529. doi:10.1029/92JB00493.

Castle, J.C., Creager, K.C., 1998. NW Pacific slab rheology, the seismicity cutoff, and the olivine to spinel phase change. *Earth Planets Space* 50, 977–985.

Caputo, M., 1986. Linear and nonlinear inverse rheologies of rocks. *Tectonophysics* 122, 53–71.

Cathles, L.M., 1975. The Viscosity of the Earth's Mantle. Princeton University Press. 386 pp.

Chen, P.-F., Bina, C.R., Okal, E.A., 2001. Variations in slab dip along the subducting Nazca Plate, as related to stress patterns and moment release of intermediate-depth seismicity and to surface volcanism. *Geochem. Geophys. Geosyst.* 2. doi:10.1029/2001GC000153.

Chatelain, J.L., Guillier, B., Gratier, J.P., 1993. Unfolding the subducting plate in the central new Hebrides island arc: geometrical argument for detachment of part of the downgoing slab. *Geophys. Res. Lett.* 20 (8), 655–658.

Chao, B.F., Gross, R.S., 2005. Did the 26 December 2004 Sumatra, Indonesia, earthquake disrupt the Earth's rotation as the mass media have said? *EOS*, 86, 1–2. Soc., 32, 203–217.

Chiarabba, C., De Gori, P., Speranza, F., 2008. The southern Tyrrhenian subduction zone: deep geometry, magmatism and Plio-Pleistocene evolution. *Earth Planet. Sci. Lett.* 268, 408–423.

Cochran, E.S., Vidale, J.E., Tanaka S., 2004. Earth tides can trigger shallow thrust fault earthquakes. *Science* 306, 1164–1166.

Conrad, C.P., Lithgow-Bertelloni, C., 2003. How mantle slabs drive plate tectonics. *Science* 298, 207–209.

Crespi, M., Cuffaro, M., Doglioni, C., Giannone, F., Riguzzi, F., 2007. Space geodesy validation of the global lithospheric flow. *Geophys. J. Int.* 168, 491–506.

Cruciani, C., Carminati, E., Doglioni, C., 2005. Slab dip vs. lithosphere age: no direct function. *Earth Planet. Sci. Lett.* 238, 298–310.

Das, S., 2004. Seismicity gaps and the shape of the seismic zone in the Band Sea region from relocated hypocenters. *J. Geophys. Res.* 109, B12303. doi:10.1029/2004JB003192.

Debayle, E., Kennett, B., Priestley, K., 2005. Global azimuthal seismic anisotropy and the unique plate-motion deformation of Australia. *Nature* 433, 509–512.

DeMets, C., Gordon, R.G., Argus, F., Stein, S., 1990. Current plate motions. *Geophys. J. Int.* 101, 425–478.

Denis, C., Schreider, A.A., Varga, P., Závoti, J., 2002. Despinning of the Earth rotation in the geological past and geomagnetic paleointensities. *J. Geodyn.* 34/5, 97–115.

Dickey, J.O., Bender, P.L., Fallor, J.E., Newhall, X.X., Ricklefs, R.L., Ries, J.G., Shelus, P.J., Veillet, C., Whipple, A.L., Wiant, J.R., Williams, J.G., Yoder, C.F., 1994. Lunar laser ranging: a continual legacy of the Apollo program. *Science* 265, 482–490.

Dickinson, W.R., 1978. Plate tectonic evolution of North Pacific rim. *J. Phys. Earth* 26, 51–519 (Suppl.).

Dingwell, D.B., Courtial, P., Giordano, D., Nichols, A.R.L., 2004. Viscosity of peridotite liquid. *Earth Planet. Sci. Lett.* 226, 127–138.

Doglioni, C., 1990. The global tectonic pattern. *J. Geodyn.* 12, 21–38.

Doglioni, C., 1993. Geological evidence for a global tectonic polarity. *J. Geol. Soc. Lond.* 150, 991–1002.

Doglioni, C., Carminati, E., Bonatti, E., 2003. Rift asymmetry and continental uplift. *Tectonics* 22 (3), 1024. doi:10.1029/2002TC001459.

Doglioni, C., Carminati, E., Cuffaro, M., Scrocca, D., 2007. Subduction kinematics and dynamic constraints. *Earth Sci. Rev.* 83, 125–175. doi:10.1016/j.earscirev.2007.04.001.

Doglioni, C., Tonarini, S., Innocenti, F., 2009. Mantle wedge asymmetries along opposite subduction zones. *Lithos.* doi:10.1016/j.lithos.2009.01.012.

Egbert, G.D., Ray, R.D., 2000. Significant dissipation of tidal energy in the deep ocean inferred from satellite altimeter data. *Nature* 405, 775–778.

Engdahl, E.R., Villaseñor, A., 2002. Global Seismicity: 1900–1999. In: Lee, W.H.K., Kanamori, H., Jennings, P.C., Kisslinger, C. (Eds.), *International Handbook of Earthquake and Engineering Seismology*, 41. Academic Press, pp. 665–690.

Engdahl, E.R., van der Hilst, R.D., Buland, R., 1998. Global teleseismic earthquake relocation with improved travel times and procedures for depth determination. *Bull. Seismol. Soc. Am.* 88, 722–743.

Espurt, N., Funicello, F., Martinod, J., Guillaume, B., Regard, V., Faccenna, C., Brusset, S., 2008. Flat subduction dynamics and deformation of the South American plate: insights from analog modeling. *Tectonics* 27, TC3011. doi:10.1029/2007TC002175.

Flasar, F., Birch, F., 1973. Energetics of core formation: a correction. *J. Geophys. Res.* 78, 6101–6103.

Forsyth, D., Uyeda, S., 1975. On the relative importance of driving forces of plate motion. *Geophys. J. R. Astron. Soc.* 43, 163–200.

Foulger, G.R., Jurdy, D.M., 2007. Plates, plumes, and planetary processes. *Geol. Soc. Am. Spec. Pap.* 430, 1–998.

Frepoli, A., Selvaggi, G., Chiarabba, C., Amato, A., 1996. State of stress in the Southern Tyrrhenian subduction zone from fault-plane solutions. *Geophys. J. Int.* 125, 879–891.

Garfunkel, Z., Anderson, C.A., Schubert, G., 1986. Mantle circulation and the lateral migration of subducted slabs. *J. Geophys. Res.* 91 (B7), 7205–7223.

Green II, H.W., Houston, H., 1995. The mechanics of deep earthquakes. *Ann. Rev. Earth Planet. Sci.* 23, 169–213.

Gripp, A.E., Gordon, R.G., 2002. Young tracks of hotspots and current plate velocities. *Geophys. J. Int.* 150, 321–361.

Gudmundsson, O., Sambridge, M., 1998. A regionalized upper mantle (RUM) seismic model. *J. Geophys. Res.* 103 (B4), 7121–7136.

Gung, Y., Panning, M., Romanowicz, B., 2003. Global anisotropy and the thickness of continents. *Nature* 422, 707–711.

Gutscher, M.-A., Malavieille, J., Lallemand, S., Collot, J.Y., 1999. Tectonic segmentation of the North Andean margin: impact of the Carnegie Ridge collision. *Earth Planet. Sci. Lett.* 168, 255–270. doi:10.1016/S0012-821X(99)00060-6.

Heinson, G., 1999. Electromagnetic studies of the lithosphere and asthenosphere. *Surv. Geophys.* 20 (4), 229–255.

- Hirth, G., Kohlstedt, D.L., 1995. Experimental constraints on the dynamics of the partially molten upper mantle, 2, Deformation in the dislocation creep regime. *J. Geophys. Res.* 100, 15441–15449.
- Hirth, G., Kohlstedt, D., 2003. Rheology of the upper mantle and the mantle wedge: a view from the experimentalists. In: Eiler, J. (Ed.), *Inside the Subduction Factory*, *Geophys. Monogr. Ser.*, vol. 138. AGU, Washington, D.C., pp. 83–105.
- Hofmeister, A.M., Criss, R.E., 2005. Earth's heat flux revised and linked to chemistry. *Tectonophysics* 395, 159–177.
- Holtzman, B.K., Groebner, N.J., Zimmerman, M.E., Ginsberg, S.B., Kohlstedt, D.L., 2003. Stress-driven melt segregation in partially molten rocks. *G3* 4, 8607. doi:10.1029/2001GC002058.
- Iriyama, J., 1977. Energy balance in the Earth's interior. *Tectonophysics* 40, 243–249.
- Isacks, B.L., Barazangi, M., 1977. Geometry of Benioff zones: lateral segmentation and downwards bending of the subducted lithosphere. In: Talwani, M., Pitman, W.C. (Eds.), *Island Arc, Deep Sea Trenches and Back-Arc Basins*, Maurice Ewing Series, vol. 1. AGU, Washington, D.C.
- Isacks, B., Molnar, P., 1971. Distribution of stresses in the descending lithosphere from a global survey of focal-mechanism solutions of mantle earthquakes. *Rev. Geophys.* 9, 103–174.
- Janle, P., Meissner, R., 1986. Structure and evolution of the terrestrial planets. *Surv. Geophys.* 8, 107–186.
- Jarrard, R.D., 1986. Relations among subduction parameters. *Rev. Geophys.* 24, 217–284.
- Jault, D., Gire, C., Le Mouél, J.J., 1988. Westward drift, core motions and exchanges of angular momentum between core and mantle. *Nature* 333, 353–356 1988.
- Jin, Z.-M., Green, H.G., Zhou, Y., 1994. Melt topology in partially molten mantle peridotite during ductile deformation. *Nature* 372, 164–167.
- Jordan, T.H., 1974. Some comments on tidal drag as a mechanism for driving plate motions. *J. Geophys. Res.* 79 (14), 2141–2142.
- Kanamori, H., 1977. The energy release in great earthquakes. *J. Geophys. Res.* 82 (20), 2981–2987.
- Kane, R.P., Trivedi, N.B., 1990. Decade fluctuations in the rotation rate of the Earth in the last 200 years. *Pageoph* 132 (4), 771–799.
- Karato, S.-I., Riedel, M.R., Yuen, D.A., 2001. Rheological structure and deformation of subducted slabs in the mantle transition zone: implications for mantle circulation and deep earthquakes. *Phys. Earth Planet. Inter.* 127, 83–108.
- Knopoff, L., 1972. Observation and inversion of surface-wave dispersion. *Tectonophysics* 13 (1–4), 497–519.
- Knopoff, L., Leeds, A., 1972. Lithospheric momenta and the deceleration of the Earth. *Nature* 237 (12), 93–95.
- Korenaga, J., Karato, S.-I., 2008. A new analysis of experimental data on olivine rheology. *J. Geophys. Res.* 113, B02403. doi:10.1029/2007JB005100.
- Kornig, H., Muller, G., 1989. Rheological model and interpretation of postglacial uplift. *Geophys. J. Int.* 98, 243–253.
- Kreemer, C., Holt, W.E., Haines, A.J., 2002. The global moment rate distribution within plate boundary zones. *Geodyn. Ser.* 30, 173–189.
- Lallemand, S., Heuret, A., Boutelier, D., 2005. On the relationships between slab dip, back-arc stress, upper plate absolute motion, and crustal nature in subduction zones. *Geochem. Geophys. Geosyst.* 6, Q09006. doi:10.1029/2005GC000917.
- Lambeck, K., 1980. In: Batchelor, G.K., Miles, J.W. (Eds.), *The Earth's Variable Rotation: Geophysical Causes and Consequences*. Cambridge University Press, Cambridge.
- Lay, T., Hernlund, J., Buffet, B.A., 2008. Core–mantle boundary heat flow. *Nature Geosci.* 1, 25–32.
- Lenci, F., Doglioni, C., 2007. On some geometric prism asymmetries. In: Lacombe, O., Lavé, J., Roure, F., Verges, J. (Eds.), *Thrust Belts and Foreland Basins: From Fold Kinematics to Hydrocarbon Systems*. Frontiers in Earth Sciences. Springer, pp. 41–60.
- Le Pichon, X., 1968. Sea-floor spreading and continental drift. *J. Geophys. Res.* 73 (12), 3661–3697.
- Lieske, C., Schmickler, B., Terasaki, H., Poe, B.T., Suzuki, A., Funakoshi, K., Ando, R., Rubie, D.C., 2005. Viscosity of peridotite liquid up to 13 GPa: implications for magma ocean viscosities. *Earth Planet. Sci. Lett.* 240, 589–604.
- Lowrie, W., 2007. *Fundamentals of Geophysics*. Cambridge University Press.
- McCarthy, D.D., Petit, G., 2004. IERS Conventions (2003), IERS Technical Note No.32, Verlag des Bundesamts für Kartographie und Geodäsie, Frankfurt am Main.
- Marcus, S.L., Chao, Y., Dickey, J.O., Gegout, P., 1998. Detection and modeling of nontidal oceanic effects on Earth's rotation rate. *Science* 281, 1656–1659.
- Marone, F., Romanowicz, B., 2007. The depth distribution of azimuthal anisotropy in the continental upper mantle. *Nature* 447, 198–202. doi:10.1038/nature05742.
- Mariotti, G., Doglioni, C., 2000. The dip of the foreland monocline in the Alps and Apennines. *Earth Planet. Sci. Lett.* 181, 191–202.
- Marquart, G., Steinberger, B., Niehuus, K., 2005. On the effect of a low viscosity asthenosphere on the temporal change of the geoid – a challenge for future gravity missions. *J. Geodyn.* 39, 493–511. doi:10.1016/j.jog.2005.04.006.
- Maslov, L.A., 1991. *Geodynamics of the Pacific Segment of the Earth*. Nauka, Moscow.
- McGeary, S., Nur, A., Ben-Avraham, Z., 1985. Special gaps in arc volcanism: the effect of collision or subduction of oceanic plateaus. *Tectonophysics* 119, 195–221. doi:10.1016/0040-1951(85)90039-3.
- Melini, D., Cannelli, V., Piersanti, A., Spada, G., 2008. Post-seismic rebound of a spherical Earth: new insights from the application of the Post-Widder inversion formula. *Geophys. J. Int.* 174 (4), 672–695.
- Milsom, J., 2005. The Vrancea seismic zone and its analogue in the Banda Arc, eastern Indonesia. *Tectonophysics* 410, 325–336.
- Molchan, G., Kronrod, T., Panza, G.F., 1997. Multi-scale seismicity model for seismic risk. *BSSA* 87 (5), 1220–1229.
- Monin, A.S., 1978. On some problems of geophysical fluid dynamics. *Proc. Natl. Acad. Sci. U.S.A.* 75 (1), 34–39.
- Moore, G.W., 1973. Westward tidal lag as the driving force of plate tectonics. *Geology* 1, 99–100.
- Nelson, T.H., Temple, P.G., 1972. Mainstream mantle convection: a geologic analysis of plate motion. *AAPG Bull.* 56 (2), 226–246.
- Oncescu, M.C., Bonjer, K.-P., 1997. A note on the depth recurrence and strain release of large Vrancea earthquakes. *Tectonophysics* 272, 291–302.
- Oncescu, M.C., Trifu, C.-I., 1987. Depth variation of moment tensor principal axes in Vrancea (Romania) seismic region. *Ann. Geophys.* 5B, 149–154.
- Panza, G.F., 1980. Evolution of the Earth's lithosphere. *NATO Adv. Stud. Inst. Newcastle*, 1979. In: Davies, P.A., Runcorn, S.K. (Eds.), *Mechanisms of Continental Drift and Plate Tectonics*. Academic Press, pp. 75–87.
- Panza, G., Raykova, R.B., Carminati, E., Doglioni, C., 2007. Upper mantle flow in the western Mediterranean. *Earth Planet. Sci. Lett.* 257, 200–214.
- Paquet, P., Dehant, V., Bruyninx, C., 1997. Earth rotation observations and their geophysical implications. *Bull. Astron. Belgrade* 156, 89–108.
- Pardo, M., Comte, D., Monfret, T., 2002. Seismotectonic and stress distribution in the central Chile subduction zone. *J. South Am. Earth Sci.* 15, 11–22. doi:10.1016/S0895-9811(02)00003-2.
- Peccerillo, A., 2005. *Plio-Quaternary Volcanism in Italy*. Petrology, Geochemistry, Geodynamics. Springer, Heidelberg. 365 pp.
- Pérez-Campos, X., Kim, Y., Husker, A., Davis, P.M., Clayton, R.W., Iglesias, A., Pacheco, J.F., Singh, S.K., Manea, V.C., Gurnis, M., 2008. Horizontal subduction and truncation of the Cocos Plate beneath central Mexico. *Geophys. Res. Lett.* 35, L18303. doi:10.1029/2008GL035127.
- Pilger, R.H., 1981. Plate reconstructions, aseismic ridges, and low-angle subduction beneath the Andes. *Geol. Soc. Am. Bull.* 92, 448–456. doi:10.1130/0016-7606(1981)92<448>
- Pollitz, F.F., Buegmann, R., Romanowicz, B., 1998. Viscosity of oceanic asthenosphere inferred from remote triggering of earthquakes. *Science* 280, 1245–1249.
- Press, F., Briggs, P., 1975. Chandler Wobble, earthquakes, rotation and geomagnetic changes. *Nature* 256, 270–273.
- Prigogine, I., Stengers, I., 1984. *Order Out of Chaos*. Bantam, New York.
- Ranalli, G., 1995. Rheology of the Earth. Chapman and Hall, pp. 1–413.
- Ranalli, G., 2000. Westward drift of the lithosphere: not a result of rotational drag. *Geophys. J. Int.* 141, 535–537.
- Ray, R., 2001. Tidal friction in the Earth and Ocean. *Journées Luxembourgeoises de Géodynamique* JLG 89th, Nov. 12–14. <http://www.ecgs.lu/>.
- Ray, R.D., Eanes, R.J., Lemoine, F.G., 2001. Constraints on energy dissipation in the earth's tide from satellite tracking and altimetry. *Geophys. J. Int.* 144, 471–480.
- Raykova, R.B., Panza, G.F., 2006. Surface waves tomography and non-linear inversion in the southeast Carpathians. *Phys. Earth Planet. Inter.* 157, 164–180.
- Reyners, M., Eberhart-Phillips, D., Stuart, G., Nishimura, Y., 2006. Imaging subduction from the trench to 300 km depth beneath the central North Island, New Zealand, with Vp and Vp/Vs. *Geophys. J. Int.* 165, 565–583. doi:10.1111/j.1365-246X.2006.02897.x.
- Ricard, Y., Doglioni, C., Sabadini, R., 1991. Differential rotation between lithosphere and mantle: a consequence of lateral viscosity variations. *J. Geophys. Res.* 96, 8407–8415.
- Rivera, L., Sieh, K., Helmberger, D., Natawidjaja, D., 2002. A comparative study of the Sumatran subduction-zone earthquakes of 1935 and 1984. *BSSA* 92 (5), 1721–1736.
- Romashkova, L.L., 2009. Global-scale analysis of seismic activity prior to 2004 Sumatra-Andaman mega-earthquake. *Tectonophysics* 470, 329–344. doi:10.1016/j.tecto.2009.02.011.
- Ruff, L., Kanamori, H., 1980. Seismicity and the subduction process. *Phys. Earth Planet. Inter.* 23, 240–252.
- Rybach, L., 1976. Radioactive heat production in rocks and its relation to other petrophysical parameters. *PAGEOPH* 114, 309–317.
- Rychert, C.A., Fischer, C.M., Rondenay, S., 2005. A sharp lithosphere–asthenosphere boundary imaged beneath eastern North America. *Nature* 436, 542–545.
- Sacks, I.S., Okada, H., 1974. A comparison of the anelasticity structure beneath western South America and Japan. *Phys. Earth Planet. Inter.* 9, 211–219. doi:10.1016/0031-9201(74)90139-3.
- Sasaki, S., Nakazawa, K., 1986. Metal-silicate fractionation in the growing Earth: energy source for the terrestrial magma ocean. *J. Geophys. Res.* 91, 9231–9238.
- Scalera, G., 2008. Great and old earthquakes against great and old paradigms – paradoxes, historical roots, alternative answers. *Adv. Geosci.* 14, 41–57.
- Scoppola, B., Boccaletti, E., Bevis, M., Carminati, E., Doglioni, C., 2006. The westward drift of the lithosphere: a rotational drag? *Bull. Geol. Soc. Am.* 118 (1/2), 199–209. doi:10.1130/B25734.1.
- Shaw, H.R., Jackson, E.D., 1973. Linear island chains in the Pacific: result of thermal plumes or gravitational anchors? *J. Geophys. Res.* 78 (35), 8634–8652.
- Stein, S., Wysession, M., 2003. *Introduction to Seismology, Earthquakes, and Earth Structure*. Blackwell Publishing.
- Stern, R.J., 2002. Subduction zones. *Rev. Geophys.* 40, 1012.
- Stevenson, D.J., 1994. Weakening under stress. *Nature* 372, 129–130.
- Syracuse, E.M., Abers, G.A., 2006. Global compilation of variations in slab depth beneath arc volcanoes and implications. *Geochem. Geophys. Geosyst.* 7, Q05017. doi:10.1029/2005GC001045.
- Thybo, H., 2006. The heterogeneous upper mantle low velocity zone. *Tectonophysics* 416, 53–79.
- Touma, J., Wisdom, J., 1994. Evolution of the Earth–Moon system. *Astron. J.* 108 (5), 1943–1961.
- Trampert, J., Deschamps, F., Resovsky, J., Yuen, D., 2004. Probabilistic tomography maps chemical heterogeneities throughout the lower mantle. *Science* 306, 853–856.
- Turcotte, D.L., Schubert, G., 2002. *Geodynamics*, Second ed. Cambridge University press.
- Twiss, R.J., Moore, E.M., 1992. *Structural Geology*. W.H. Freeman and Compan, New York. 531 pp.
- Uyeda, S., Kanamori, H., 1979. Back-arc opening and the mode of subduction. *J. Geophys. Res.* 84 (B3), 1049–1061.
- Varga, P., 2006. Temporal variation of geodynamical properties due to tidal friction. *J. Geodyn.* 41, 140–146.

- Varga, P., Gambis, D., Bus, Z., Bizouard, C., 2005. The Relation Between the Global Seismicity and the Rotation of the Earth, Observatoire de Paris, Systèmes de référence temps-espace UMR8630/CNRS, pp. 115–121.
- Vasco, D.W., Johnson, L.R., Marques, O., 2003. Resolution, uncertainty, and whole Earth tomography. *J. Geophys. Res.* 108. doi:10.1029/2001JB000412.
- Vassiliou, M.S., Hager, B.H., Raefsky, A., 1984. The distribution of earthquakes with depth and stress in subducting slabs. *J. Geodyn.* 1, 11–28.
- Verhoogen, J., 1980. *Energetics of the Earth*, University of California, National Academy of Science.
- Vinnik, L., Singh, A., Kiselev, S., Ravi Kumar, M., 2007. Upper mantle beneath foothills of the western Himalaya: subducted lithospheric slab or a keel of the Indian shield? *Geophys. J. Int.* 171, 1162–1171. doi:10.1111/j.1365-246X.2007.03577.x.
- Wang, Q.-L., Chen, Y.-T., Cui, D.-X., Wang, W.-P., Liang, W.-F., 2000. Decadal correlation between crustal deformation and variation in length of day of the Earth. *Earth Planets Space* 52, 989–992.
- Wortel, M.J.R., 1984. Spatial and temporal variations in the Andean subduction zone. *J. Geol. Soc.* 141 (5), 783–791.
- Walter, M.J., Trønnes, R.G., 2004. Early Earth differentiation. *Earth Planet. Sci. Lett.* 225, 253–269.
- Wilcock, W.S.D., 2001. Tidal triggering of microearthquakes on the Juan de Fuca Ridge. *Geophys. Res. Lett.* 28 (20), 3999–4002.
- Yoder, C.F., Williams, J.G., Parke, M.E., 1981. Tidal variations of Earth rotation. *J. Geophys. Res.* 86, 881–891.
- Zhang, Y.-S., Tanimoto, T., 1993. High-resolution global upper mantle structure and plate tectonics. *J. Geophys. Res.* 98 (B6), 9793–9823.
- Zschau, J., 1986. Tidal friction in the solid Earth: constraints from the Chandler wobble period. In: Anderson, A.J., et al. (Ed.), *Space Geodesy and Geodynamics*, pp. 315–344.